Biological Sciences

College of Science, Technology, and Health

11-2000

# Does a rigid body limit maneuverability?

Jeffrey A. Walker
*University of Southern Maine*, walker@usm.maine.edu

Follow this and additional works at: http://digitalcommons.usm.maine.edu/biology

Part of the Biology Commons

# DOES A RIGID BODY LIMIT MANEUVERABILITY?

JEFFREY A. WALKER*

*Department of Zoology, Field Museum of Natural History, 1400 S. Lake Shore Drive, Chicago, IL 60605, USA*

*Present address: Department of Biological Sciences, University of Southern Maine, Box 9300, Portland, ME 04104-9300, USA
(e-mail: walker@usm.maine.edu)

## Summary

Whether a rigid body limits maneuverability depends on how maneuverability is defined. By the current definition, the minimum radius of the turn, a rigid-bodied, spotted boxfish *Ostracion meleagris* approaches maximum maneuverability, i.e. it can spin around with minimum turning radii near zero. The radius of the minimum space required to turn is an alternative measure of maneuverability. By this definition, *O. meleagris* is not very maneuverable. The observed space required by *O. meleagris* to turn is slightly greater than its theoretical minimum but much greater than that of highly flexible fish. Agility, the rate of turning, is related to maneuverability. The median- and pectoral-fin-powered turns of *O. meleagris* are slow relative to the body- and caudal-fin-powered turns of more flexible fish.

Key words: swimming, turning performance, agility, curvature, kinematics, body stiffness, manoeuvrability, boxfish, *Ostracion meleagris*.

## Introduction

Most literature on the locomotion of fishes has focused on the maximum performance of either rectilinear swimming at uniform velocities or the fast-start escape response. In contrast, routine swimming performance is poorly understood, despite the greater frequency of routine swimming relative to the higher-performance behaviors (Webb, 1994a,b). Routine swimming in many fish species consists of frequent maneuvers, including turning laterally (yaw) and dorsoventrally (pitch), rolling, starting, braking and hovering (Breder, 1926). Most studies of animal maneuvering performance have focused on lateral turning. In fact, Norberg and Rayner (1987) formally defined maneuverability as the ability to turn in a confined space and have used the length-specific minimum radius of the turning path ($r_{path}/L$, where $L$ is total body length) as a measure of this performance. Webb (1994a) has advocated this limited definition of maneuverability for fishes.

Morphologies that facilitate or limit turning have been widely discussed, but the effects of many design features on turning performance remain poorly resolved (Gerstner, 1999; Schrank and Webb, 1998; Schrank et al., 1999; Webb et al., 1996). It has been suggested that a stiff body limits turning performance (Aleev, 1969; Fish, 1997, 1999). The results of several studies are consistent with this hypothesis. The $r_{path}/L$ of a fish with a relatively stiff body, the yellowfin tuna *Thunnus albacores* (0.47), is an order of magnitude greater than the relative turning radii of two fish with more flexible bodies, the knifefish *Xenomystus nigri* (0.065) and the angelfish *Pterophyllum eimekei* (0.055) (Blake et al., 1995; Domenici

and Blake, 1997). Fish (1997) showed that the more flexible-bodied sea lion *Zalophus californianus* had a smaller $r_{path}/L$ than seven more stiff-bodied species of cetaceans. Finally, Fish (1999) showed that the rigid-bodied whirligig beetle *Dineutus horni* has a higher $r_{path}/L$ than more flexible fishes and aquatic mammals.

Nevertheless, Blake (1977) illustrated turning maneuvers of apparently small radii in two fishes with rigid bodies, the boxfishes (Ostraciidae) *Lactoria cornuta* and *Tetrasomus gibbosus*. Boxfishes are shallow-water, temperate and tropical fishes that are encased by a carapace of thickened, sutured scales modified into bony plates (Randall, 1972; Tyler, 1980). Because of this rigid armor, boxfishes cannot undulate their body anterior to the caudal peduncle. Consequently, boxfishes power both slow rectilinear swimming and turning maneuvers by oscillating or undulating the fan-shaped pectoral, dorsal and anal fins (Blake, 1977).

If boxfish can indeed turn with a small $r_{path}$, this would suggest that $r_{path}$ is not a good measure of the actual radius of the space required to turn. A turn requires both the rotation of the animal and a translation of the center of rotation along a turning path. Letting $r_e$ equal the effective radius of the turning animal (half the maximum projected diameter of the animal normal to the turning path), the minimum radius of the space required to turn, $r_{space}$, is $r_e+r_{path}$. For a rigid-bodied animal turning with $r_{path}=0$ (spinning with no translation), the minimum $r_{space}$ is $L/2$. At the least, a flexible fish with the same $L$ and $r_{path}$ as a rigid fish should be able to turn in a smaller space than the rigid fish simply by having a smaller $r_e$.

Both measures of maneuverability, $r_{path}$ and $r_{space}$, are important for the biology of fishes (see Discussion). To test whether and how body stiffness limits these two aspects of maneuverability, I measured both $r_{path}$ and $r_{space}$ in routine turns of a spotted boxfish *Ostracion meleagris* (Randall, 1972).

## Materials and methods

A single, female *Ostracion meleagris* (Fig. 1) was purchased from a wholesaler in Chicago (total length, $L=11.6$ cm). The fish was allowed 2 days to acclimate to the test tank, a 37.8 l aquarium fitted with a mirror oriented at 45 ° to the tank bottom. Water temperature was 25 °C. Dorsal views of turning sequences were filmed with a Red Lake high-speed digital camera at 125 Hz and saved as AVI files. There were no explicit attempts to elicit turning behavior by startling the fish.

AVI files were converted to Apple QuickTime format and digitized in a version of the public-domain NIH Image software (developed at the US National Institutes of Health and available on the Internet at http://rsb.info.nih.gov/nih-image/) modified to facilitate the digitization of landmarks (available from the author upon request). Twelve turning sequences in which there was little dorsoventral translation were analyzed. Both sharp and gradual turns were analyzed. All analyzed turns were preceded by forward swimming and were through a cumulative turning angle of >150 °. Four landmarks were digitized every fifth frame (Fig. 1): the tip of the snout, a spot on the dorsal midline immediately anterior to the dorsal fin, the base of the caudal fin and the posterior tip of the caudal fin.

The center of rotation was determined from the snout and dorsal fin landmarks. One hundred equally spaced landmarks along the line segment connecting the snout and dorsal fin landmarks were constructed. The location of the center of rotation was estimated as the constructed landmark that traveled the smallest cumulative distance over the turning sequence. The instantaneous curvature, $\kappa$, which is a measure of the rate of rotation of the tangent to the path, was computed along the turning path by the parametric function:

$$\kappa = |x'y'' - y'x''|/[(x')^2 + (y')^2]^{3/2},$$

where $'$ and $''$ reflect the first and second derivative of $x$ or $y$ with respect to distance along the turning curve. First and second derivatives of $x$ and $y$ were estimated using a quintic spline (Walker, 1998a) in the software QuicKurve (Walker, 1998b). The instantaneous radius of the turning curve, $r_{path}$, is simply the reciprocal of $\kappa$.

The snout and caudal fin tip paths were used to estimate the boundaries of the turning space. These boundaries were computed as the maximum perpendicular distance to either side of the midline axis in the initial frame (Fig. 2). These distances were found by rotating the snout and caudal fin tip landmarks by the angle between the midline axis of the first frame and a positive $x$ vector. $r_{space}$ was then calculated as half the difference between the maximum and minimum $y$ coordinates.

In addition to these two turning radii, several other variables were measured. Instantaneous turn angle, $\theta$, was estimated as the angle between the midline segment connecting the snout and dorsal fin at time zero and the segment at time $t$. $\theta$ was
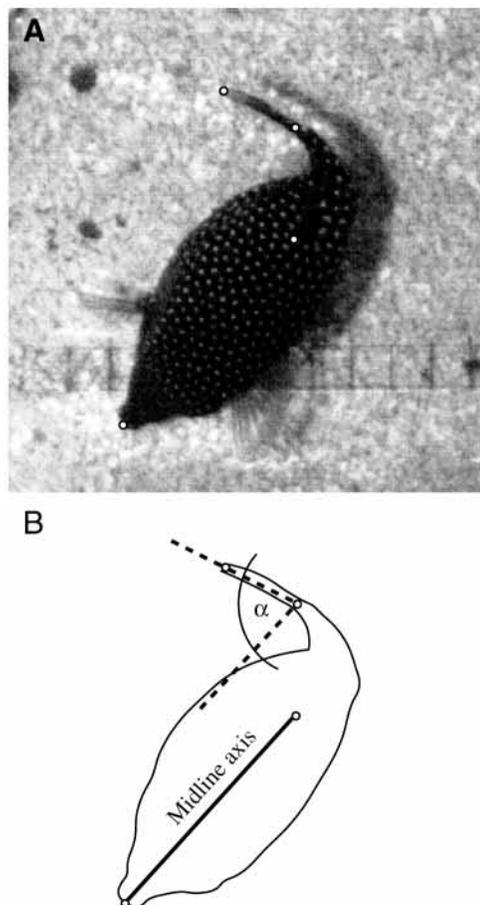


Fig. 1. (A) Dorsal view of a female *Ostracion meleagris*. The four landmarks digitized are illustrated with white circles. (B) Construction of the midline axis of the fish and the angle, $\alpha$, between the axis of the caudal fin and the median axis.
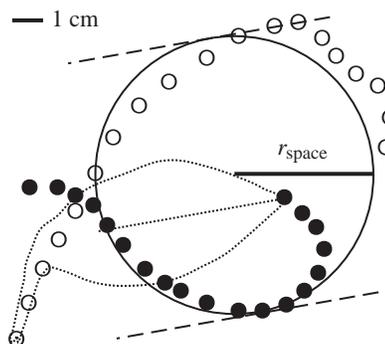


Fig. 2. Visual definition of $r_{space}$, the radius of the circle that fits the space defined by the two lines parallel to the midline axis at the start of the turn and running through the two points reflecting maximum excursion of the body to either side of the starting midline axis.

differentiated with respect to time using a quintic spline algorithm (Walker, 1998a) to determine the turning velocity, $\omega$. A normal acceleration coefficient, $C_g$, was computed as $v^2/r_{path}\boldsymbol{g}$ (Bandyopadhyay, 1997), where $v$ is the tangential velocity at $\kappa_{max}$ and $\boldsymbol{g}$ is the acceleration due to gravity. Finally, the instantaneous angle, $\alpha$, of the caudal fin, relative to the midline axis of the body was measured.

### Results

Turn magnitudes ranged from 153.2 to 250.4° (Table 1). The distance traveled by the center of rotation ranged from 5.2 to 15.8 cm (0.44–1.36$L$). The time for these turns ranged from 1.04 to 2.76 s. Mean turn rate ranged from 76.1 to 147° s$^{-1}$, while mean tangential velocity ranged from 2.7 to 8.1 cm s$^{-1}$ (0.23–0.7 $L$ s$^{-1}$).

Although *O. meleagris* can perform hovering turns (rotation of the body without translation of the center of rotation), all analyzed turns included both translational and rotational components. Turning paths were not along the arc of a circle, which would require constant $\kappa$ throughout the turn, but were characterized by an initial section with a low $\kappa$, a middle loop with a high $\kappa$, and a final section with a low $\kappa$ (Figs 3, 4). While most of the sequences had single peaks of maximum curvature, three of the 12 sequences had two peaks of high curvature (Table 1; Fig. 4). In these double-peak turns, the loop section was characterized by an initial sharp 90° turn, followed by a short, straight path and then by a second sharp 90° turn. The
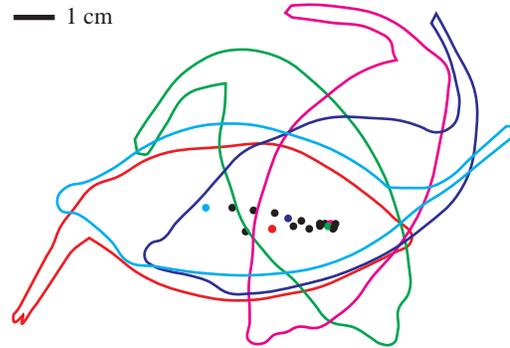


Fig. 3. Displacement of the center of rotation over time for the sequence with $r_{path}/L=0.0005$, where $r_{path}$ is the minimum radius of the turning path and $L$ is total body length (see Table 1). The center of rotation points are illustrated at 0.08 s intervals. The outlines of the body are illustrated at 0.32 s intervals.

fish rotated during the intervals with low curvature, indicating that the body was spinning while sliding, or slipping, through the water (Fig. 3). $\kappa$ was not constant during the loop of high curvature but instead peaked approximately half-way through the loop. $r_{path}$ was taken as the inverse of maximum curvature, $\kappa_{max}$ (Table 1). Minimum $r_{path}/L$ of the loop section ranged from 0.0005 to 0.11. Minimum effective length, $L_e$, during a turn was 8.3 cm. Minimum $r_{space}/L$ ranged from 0.38 to 0.57, while $r_{space}/L_e$, which has a theoretical minimum of 0.5, ranged from 0.53 to 0.8.

Table 1. *Turning statistics for the 12 analyzed turning sequences*

| Type | Period (s) | $\Delta_T$ (cm) | $\theta_T$ (degrees) | $\alpha_{min}$ (degrees) | $U_o$ ($L$ s$^{-1}$) | $U_{min}$ ($L$ s$^{-1}$) | $r_{path}/L$ | $r_{space}/L$ | $\omega_{max}$ (° s$^{-1}$) | $\omega_{avg}$ (° s$^{-1}$) | $C_g$ |
|---|---|---|---|---|---|---|---|---|---|---|---|
| Double | 1.40 | 6.50 | 166.7 | 58.4 | 0.48 | 0.31 | 0.0802 | 0.47 | 153.1 | 119.1 | 0.0140 |
| Single | 1.04 | 7.40 | 153.2 | 46.9 | 1.14 | 0.09 | 0.0103 | 0.43 | 218.4 | 147.3 | 0.0474 |
| Single | 1.28 | 5.16 | 171.2 | 55.1 | 0.57 | 0.12 | 0.0140 | 0.40 | 148.7 | 133.8 | 0.0128 |
| Double | 2.12 | 14.07 | 250.4 | 81.2 | 0.67 | 0.35 | 0.0914 | 0.50 | 179.4 | 118.1 | 0.0158 |
| Single | 1.44 | 5.95 | 194.5 | 59.6 | 0.80 | 0.08 | 0.0005 | 0.40 | 200.5 | 135.0 | 0.1625 |
| Double | 1.96 | 15.82 | 222.8 | 89.9 | 0.58 | 0.41 | 0.1121 | 0.57 | 197.4 | 113.7 | 0.0193 |
| Single | 2.40 | 11.80 | 191.4 | 68.0 | 0.64 | 0.07 | 0.0024 | 0.39 | 106.8 | 79.7 | 0.0822 |
| Single | 1.76 | 10.03 | 176.8 | 56.6 | 0.80 | 0.21 | 0.0336 | 0.42 | 182.0 | 100.4 | 0.0181 |
| Single | 2.76 | 8.24 | 210.0 | 59.5 | 0.62 | 0.11 | 0.0179 | 0.38 | 132.9 | 76.1 | 0.0133 |
| Single | 2.52 | 6.93 | 212.1 | 58.4 | 0.61 | 0.10 | 0.0084 | 0.41 | 140.6 | 84.2 | 0.0142 |
| Single | 2.04 | 5.96 | 165.3 | 62.2 | 0.46 | 0.09 | 0.0059 | 0.44 | 116.9 | 81.0 | 0.0151 |
| Single | 1.84 | 6.47 | 170.6 | 58.2 | 0.62 | 0.11 | 0.0129 | 0.44 | 137.6 | 92.7 | 0.0106 |

Type refers to turns with one or two curvature peaks.
Period is the time required for the turn.
$\Delta_T$ is the total, cumulative distance traveled by the center of rotation during the turn.
$\theta_T$ is the total, cumulative rotation angle of the midline axis of the body.
$\alpha_{min}$ is the minimum angle between the caudal fin and the midline axis.
$U_o$ is the tangential velocity of the center of rotation entering the turn.
$U_{min}$ is the minimum tangential velocity of the center of rotation during the turn.
$r_{path}/L$ is the length-specific turning radius, where $L$ is total body length.
$r_{space}/L$ is the length-specific radius of the space required to turn.
$\omega_{max}$ is the maximum angular velocity of the midline axis.
$\omega_{avg}$ is the average angular velocity over the turn.
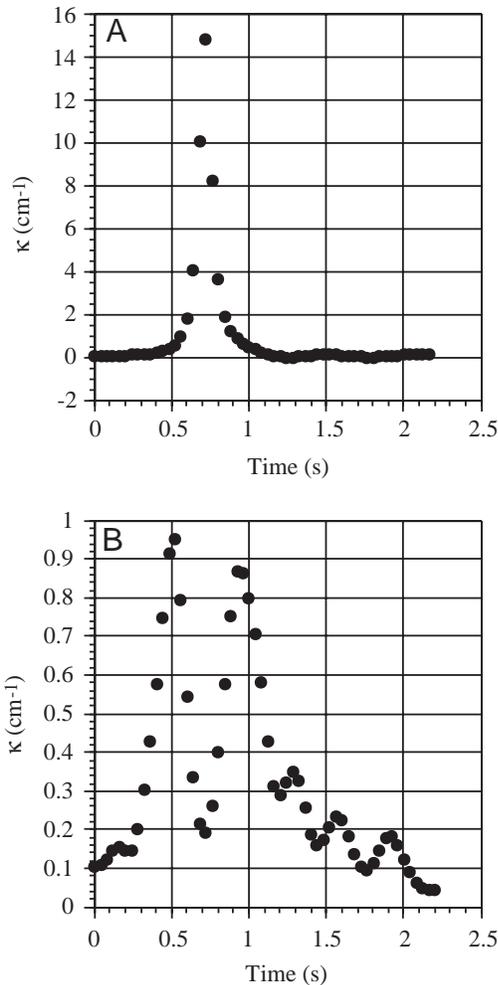$C_g$ is the peak normal acceleration standardized by $\boldsymbol{g}$.

Fig. 4. Curvature, κ, for (A) a sequence with a single κ peak and (B) a sequence with a double κ peak.

Angular velocities changed throughout the turn. Peak ω, or $\omega_{max}$, ranged from 107 to 218° s$^{-1}$. $\omega_{max}$ always occurred at or close to $t_{max}$, the time at which the turning curvature reaches its maximum. Tangential velocities changed throughout the turn, generally reaching a minimum near $t_{max}$. $C_g$ values, which ranged from 0.01 to 0.16, were computed using the tangential velocity at $t_{max}$.

Howland (1974) suggested that $r_{path}$ should be independent of the tangential velocity entering the turn. Indeed, neither $r_{path}$ nor $r_{space}$ was correlated with the tangential velocity entering the turn ($r_{path}$, $r=-0.24$, $P=0.43$; $r_{space}$, $r=-0.17$, $P=0.59$). In contrast, both $r_{path}$ and $r_{space}$ were correlated with the tangential velocity at $t_{max}$ ($r_{path}$, $r=0.96$, $P<0.0001$; $r_{space}$, $r=0.87$, $P=0.0003$). This correlation is expected; at the limit, when $\kappa_{max}$ is infinite, the tangential velocity must fall to zero as the body stops and reverses direction. $\omega_{max}$ was correlated with the tangential velocity entering the turn ($r=0.69$, $P=0.01$) but not with the tangential velocity at $t_{max}$ ($r=0.49$, $P=0.11$) nor with either $r_{path}$ or $r_{space}$ ($r_{path}$, $r=0.36$, $P=0.25$; $r_{space}$, $r=0.41$, $P=0.18$).

The angle, α, of the caudal fin relative to the midline axis of the body changed throughout the stroke, reaching a minimum, $\alpha_{min}$, at or near the time of $\omega_{max}$. In some turns, the minimum formed a distinct inverted peak, while in others the minimum was within a broad inverted plateau. $\alpha_{min}$ ranged from 46.9 to 68° for turns with single high-curvature peaks (Table 1). $\alpha_{min}$ was 58.4°, 81.2° and 89.9° for the turns with two curvature peaks. Within turns, correlations between α and ω ranged between −0.8 and −0.94. Among turns, $\alpha_{min}$ was significantly correlated with $r_{path}$ and $r_{space}$ ($r_{path}$, $r=0.74$, $P=0.006$; $r_{space}$, $r=0.75$, $P=0.005$). Excluding the double high-curvature turns, $\alpha_{min}$ was significantly correlated with $\omega_{max}$ ($r=-0.77$, $P=0.015$). These correlations suggest that the *O. meleagris* is partially controlling its turning kinematics by using the caudal fin as a rudder.

## Discussion

The single *O. meleagris* individual sufficiently demonstrated that a rigid-bodied fish can perform lateral turning maneuvers of approximately 180° during forward locomotion with minimum turning radii, $r_{path}$, approaching zero. This observation should not surprise anyone who has watched boxfish swim. The *O. meleagris* turns question the use of $r_{path}$ as a measure of turning space. $r_{path}$ will only approximate the radius of the actual turning space if the midline axis of the fish follows the turning path throughout the turn. For tight turns, the midline axis of the *O. meleagris* cannot follow the turning curve because of its rigid body. Instead, the snout and caudal fin tip paths sweep out much larger spaces than the center-of-rotation path (Fig. 3).

The actual radius of the space required to turn is captured by $r_{space}$. The theoretical minimum $r_{space}$ for a turn is half the effective length of the fish, where the effective length is the major axis of the bent body. This minimum assumes that the fish is bent with constant curvature along its length and can maintain this curvature throughout the turn. A fish could turn with still smaller $r_{space}$ if it effectively folded its body by passing a single, short wave of very high curvature down its body, as seems to occur in turning maneuvers of elongated, highly flexible fishes.

In the *O. meleagris* examined here, observed $r_{space}$ for the turns with single high-curvature peaks ranged from 6 to 60% above the theoretical minimum. The observed values are higher than the minimum value, even for the turns with low $r_{path}$, because the fish failed to maintain a low $r_{path}$ throughout the turn. Casual observations suggest that *O. meleagris* can maintain a low $r_{path}$ throughout a turn of 180° (and much higher), but these behaviors were not captured on digital video.

How do the minimum $r_{path}/L$ (0.0005) and $r_{space}/L$ (0.38) measured for this individual compare with those of other animals? For the stiff-bodied whirligig beetle *Dineutus horni*, minimum $r_{path}/L$ was measured as 0.24 (Fish, 1999). For more flexible animals, $r_{path}/L$ can be much lower. Mean $r_{path}/L$ for the angelfish *Pterophylum eimekei* performing fast-start escape

maneuvers was 0.065, but a minimum value has not been reported (Domenici and Blake, 1991). Domenici and Blake (1997) report an $r_{path}/L$ of 0.055 for the knifefish *Xenoystus nigri*. Gerstner (1999) found minimum values of $r_{path}/L$ between 0.02 and 0.05 for the median- and paired-fin (MPF)-powered turns and between approximately 0 and 0.05 for body- and caudal-fin (BCF)-powered turns of four species of coral reef fishes (foureye butterflyfish, *Chaetodon capistratus*; beaugregory damselfish, *Stegastes leucostictus*; ocean surgeonfish, *Acanthurus bahanieusis*; bluehead wrasse, *Thalassoma bifasciatus*). Minimum $r_{path}/L$ was 0.09 for the California sea lion *Zalophus californianus* (Fish, 1997).

Turning curvatures along a turning path in the *O. meleagris* were not constant but were characterized by a sharp maximum approximately half-way through the turn. Among different animals, there is a continuum of turning styles, from quasi-uniform curvature turns along an arc of a circle to the highly non-uniform curvature turns of the boxfish. Unfortunately, there are not enough quantitative data from the literature to explore the relationship between maximum curvature within a path and the variability of curvatures along the path.

The only $r_{space}$ values that I have found reported in the literature are from Schrank et al. (1999), who cleverly measured the minimum space required to turn by coercing fish to turn within tubes of different diameter. For turns of 180°, mean $r_{space}/L$ was approximately 0.11 for goldfish (*Carassius auratus*), 0.24 for silver dollar (*Metynnis hypsauchen*) and 0.26 for angelfish (*Pterophylum scalare*). The highest value, that for *P. scalare*, is more than three standard errors below 0.36, which is the minimum theoretical value for the individual *O. meleagris* analyzed here. Clearly, the flexible fishes can turn in smaller spaces than the rigid boxfish.

Webb (1994a) defined agility as the ability to quickly reorient the body and suggested turning rate, $\omega$, as a measure of agility. The *O. meleagris* performed slow turns; the maximum instantaneous turning rate was $218°\,s^{-1}$, while the maximum turning rate averaged over the entire turn, $\omega_{avg}$, was $147°\,s^{-1}$. By comparison, $\omega_{avg}$ for the whirligig beetle ranged from 400 to $4428°\,s^{-1}$. $\omega_{avg}$ for the four coral reef fishes in the study of Gerstner (1999) ranged from approximately 100 to $1200°\,s^{-1}$ for MPF turns and from approximately 650 to $9200°\,s^{-1}$ for BCF turns. The sea lion *Z. californianus* turned at rates ranging from 150 to $690°\,s^{-1}$ (Fish, 1997). Five of the seven cetaceans (with generally stiffer bodies than the sea lion) analyzed by Fish (1997) had low $\omega_{avg}$, ranging between 25 and $200°\,s^{-1}$, although one of the species (the white-sided dolphin *Lagenorhynchus obliquidens*) had a maximum $\omega_{avg}$ of $453°\,s^{-1}$.

In a comparison of $\omega_{avg}$ across a broad size range of flexible, aquatic animals, Fish (1999) showed that $\omega_{avg}$ decreases with $L$. The $\omega_{avg}$ of two stiff-bodied vehicles, the whirligig beetle and the submarine *USS Albacor*e, were six and eight times slower than the expected $\omega_{avg}$ of flexible animals (based on a deviation from the least-squares regression). In comparison, the maximum $\omega_{avg}$ for the *O. meleagris* was 26 times slower

than the expected $\omega_{avg}$. The measurement of maximum $\omega_{avg}$ for boxfish, in general, was not the goal of this study and there was no attempt to stimulate faster turns. The turning rate data are comparable, then, with the values for the reef fishes (Gerstner, 1999), cetaceans (Fish, 1997) and the whirligig beetle (Fish, 1999), but not with the fast-start escape values (Domenici and Blake, 1997), for which maximal performance is expected. Variation in $\omega_{avg}$ among multiple individuals or species of Ostraciidae was also not measured. Nevertheless, the available *O. meleagris* data, in combination with those of Fish (1999), are consistent with the hypothesis that a stiff body limits agility (Fish, 1997, 1999).

There are at least three reasons why the rigid body of the boxfish should limit agility. First, the bony exoskeleton precludes the myotomal muscles from bending the cranial end of the body into the turn and the caudal end of the body away from the turn. Second, the rigid body results in a relatively high pressure drag resisting rotation because the angle of attack between the body and the local flow is close to 90° along the entire length of the body. Finally, the inability to bend the body does not allow the fish to reduce the body's second moment of area about the dorsoventral rotational axis, resulting in high inertial resistance to rotation.

Using $r_{path}$ as a measure of maneuverability, the *O. meleagris* was maximally maneuverable despite its stiff body. Using $r_{space}$, the *O. meleagris* was a poor maneuverer relative to more flexible fish. Importantly, both performance variables are important measures of maneuverability in its broader sense. $r_{space}$ should be associated with the ability effectively to exploit confined spaces created by complex structure, such as the vegetated margins of lakes and rock and coral reefs. The ability to rotate with a low $r_{path}$, in contrast, allows an individual precise control of its orientation, which could be important for sampling individual prey, especially in environments with rapidly changing flow velocities.

Boxfish power turns by the combined oscillation and undulation of the pectoral, dorsal and anal fins (Blake, 1977). The high correlations between $\alpha$ and $\omega$ within turns and between $\alpha_{min}$ and $r_{path}/L$ among turns suggest that the caudal fin has a large influence on turning control by effectively acting as a rudder (Blake, 1977). The multiple control devices employed by maneuvering boxfish allow precise control of position and orientation, despite the rigid body.

Many reef fishes escape predation by rapidly seeking refuge within narrow spaces created by corals (Hixon and Beets, 1993), a behavior that is facilitated by extremely flexible (Hixon and Beets, 1993) or narrow (Webb et al., 1996) bodies. While the bony exoskeleton results in a rigid body that appears to limit the ability of boxfish to turn rapidly and in tight spaces, two behaviors necessary for effective refuging, the combination of the exoskeleton and the stress-induced secretion of ostracitoxin (Sancho, 1998; Thompson, 1964), provide an effective (but not perfect, see Sudekum et al., 1991), non-locomotor, anti-predator mechanism. By circumventing the need to refuge, the boxfish avoids the potential costs of refuging behavior (Godin, 1997).

## References

**Aleev, Y. G.** (1969). *Function and Gross Morphology in Fish*. Jerusalem: Israel Program for Scientific Translations. 268pp.

**Bandyopadhay, P. R., Castano, J. M., Rice, J. Q., Philips, B., Nedderman, W. H. and Macy, W. K.** (1997). Low speed maneuvering hydrodynamics of fish and small underwater vehicles. *J. Fluids Eng.* **119**, 136–144.

**Blake, R. W.** (1977). On ostraciiform locomotion. *J. Mar. Biol. Ass. UK* **57**, 1047–1055.

**Blake, R. W., Chatters, L. M. and Domenici, P.** (1995). Turning radius of yellowfin tuna (*Thunnus albacares*) in unsteady swimming manoevres. *J. Fish Biol.* **46**, 536–538.

**Breder, C. M, Jr** (1926). The locomotion of fishes. *Zoologica* **4**, 159–291.

**Domenici, P. and Blake, R. W.** (1991). The kinematics and performance of the escape response in the angelfish (*Pterophyllum eimekei*). *J. Exp. Biol.* **156**, 187–205.

**Domenici, P. and Blake, R. W.** (1997). The kinematics and performance of fish fast-start swimming. *J. Exp. Biol.* **200**, 1165–1178.

**Fish, F. E.** (1997). Biological designs for enhanced maneuverability: analysis of marine mammal performance. In *Tenth International Symposium on Unmanned Untethered Submersible Technology*, pp. 109–117. Durham, NH: Autonomous Undersea Systems Institute.

**Fish, F. E.** (1999). Performance constraints on the maneuverability of flexible and rigid biological systems. In *Eleventh International Symposium on Unmanned Untethered Submersible Technology*, pp. 394–406. Durham, NH: Autonomous Undersea Systems Institute.

**Gerstner, C. L.** (1999). Maneuverability of four species of coral-reef fish that differ in body and pectoral-fin morphology. *Can. J. Zool.* **77**, 1102–1110.

**Godin, J.-G. J.** (1997). Evading predators. In *Behavioral Ecology of Teleost Fishes* (ed. J.-G. J. Godin), pp. 191–236. New York: Oxford University Press.

**Hixon, M. A. and Beets, J. P.** (1993). Predation, prey refuges and the structure of coral-reef fish assemblages. *Ecol. Monogr.* **63**, 77–101.

**Howland, H. C.** (1974). Optimal strategies for predator avoidance: the relative importance of speed and manoeuvrability. *J. Theor. Biol.* **47**, 333–350.

**Norberg, U. and Rayner, J. M. V.** (1987). Ecological morphology and flight in bats (Mammalia: Chiroptera): wing adaptations, flight performance, foraging strategy and echolocation. *Phil. Trans. R. Soc. Lond. B* **316**, 335–427.

**Randall, J. E.** (1972). The Hawaiian trunkfishes of the Genus Ostracion. *Copeia* **1972**, 756–768.

**Sancho, G.** (1998). Factors regulating the height of spawning ascents in trunkfishes (Ostraciidae). *J. Fish Biol.* **53**A, 94–103.

**Schrank, A. J. and Webb, P. W.** (1998). Do body and fin form affect the abilities of fish to stabilize swimming during maneuvers through vertical and horizontal tubes? *Env. Biol. Fish.* **53**, 365–371.

**Schrank, A. J., Webb, P. W. and Mayberry, S.** (1999). How do body and paired-fin positions affect the ability of three teleost fishes to maneuver around bends? *Can. J. Zool.* **77**, 203–210.

**Sudekum, A. E., Parrish, J. D., Radtke, R. L. and Ralston, S.** (1991). Life history and ecology of large jacks in undisturbed, shallow, oceanic communities. *Fish. Bull.* **89**, 493–513.

**Thompson, D. A.** (1964). Ostracitoxin: an ichthyotoxic stress secretion of the boxfish, *Ostracion lentiginosus*. *Science* **146**, 244–245.

**Tyler, J. C.** (1980). Osteology, phylogeny and higher classification of the fishes of the order Plectognathi (Tetraodontiformes). *NOAA Technical Report NMFS Circular* **434**.

**Walker, J. A.** (1998a). Estimating velocities and accelerations of animal locomotion: a simulation experiment comparing numerical differentation algorithms. *J. Exp. Biol.* **201**, 981–995.

**Walker, J. A.** (1998b). QuicKurve. [WWW document] http://jaw.fmnh.org/software/qs.html: Department of Zoology, Field Museum of Natural History, Chicago, USA.

**Webb, P. W.** (1994a). The biology of fish swimming. In *Mechanics and Physiology of Animal Swimming* (ed. L. Maddock, Q. Bone and J. M. V. Rayner), pp. 45–62. Cambridge: Cambridge University Press.

**Webb, P. W.** (1994b). Exercise performance of fish. In *Comparative Vertebrate Exercise Physiology: Phyletic Adaptations* (ed. J. H. Jones), pp. 1–49. San Diego: Academic Press.

**Webb, P. W., LaLiberte, G. D. and Schrank, A. J.** (1996). Do body and fin form affect the maneuverability of fish traversing vertical and horizontal slits? *Env. Biol. Fish.* **46**, 7–14.